Biosensors and Bioelectronics 85 (2016) 1–7

Contents lists available at ScienceDirect

Biosensors and Bioelectronics

journal homepage: www.elsevier.com/locate/bios

Portable, one-step, and rapid GMR biosensor platform with smartphone interface

Joohong Choi [a,1], Adi Wijaya Gani [a,1], Daniel J.B. Bechstein [b], Jung-Rok Lee [b], Paul J. Utz [c], Shan X. Wang [a,d,e,*]

[a] Department of Electrical Engineering, Stanford University, Stanford, CA 94305, USA
[b] Department of Mechanical Engineering, Stanford University, Stanford, CA 94305, USA
[c] School of Medicine, Division of Immunology and Rheumatology, Stanford University, Stanford, CA 94305, USA
[d] Department of Material Science, Stanford University, Stanford, CA 94305, USA
[e] Geballe Laboratory for Advanced Materials, Stanford University, McCullough Building, Room 351, 476 Lomita Mall, Stanford, CA 94305–4045, USA

ARTICLE INFO

Article history:
Received 26 February 2016
Received in revised form
14 April 2016
Accepted 18 April 2016
Available online 19 April 2016

Keywords:
Point of care
Portable and rapid diagnostics
Smartphone integration
GMR sensor
One-step magnetic immunoassay
Magnetic nanoparticle

ABSTRACT

Quantitative immunoassay tests in clinical laboratories require trained technicians, take hours to complete with multiple steps, and the instruments used are generally immobile–patient samples have to be sent in to the labs for analysis. This prevents quantitative immunoassay tests to be performed outside laboratory settings. A portable, quantitative immunoassay device will be valuable in rural and resource-limited areas, where access to healthcare is scarce or far away. We have invented Eigen Diagnosis Platform (EDP), a portable quantitative immunoassay platform based on Giant Magnetoresistance (GMR) biosensor technology. The platform does not require a trained technician to operate, and only requires one-step user involvement. It displays quantitative results in less than 15 min after sample insertion, and each test costs less than US$4. The GMR biosensor employed in EDP is capable of detecting multiple biomarkers in one test, enabling a wide array of immune diagnostics to be performed simultaneously. In this paper, we describe the design of EDP, and demonstrate its capability. Multiplexed assay of human immunoglobulin G and M (IgG and IgM) antibodies with EDP achieves sensitivities down to 0.07 and 0.33 nanomolar, respectively. The platform will allow lab testing to be performed in remote areas, and open up applications of immunoassay testing in other non-clinical settings, such as home, school, and office.

1. Introduction

Laboratory health diagnostic platforms have been continuously advancing, taking advantage of a wide variety of transducing mechanisms such as optics (Fan et al., 2008; Haes and Van Duyne, 2002; Kneipp et al., 2010), magnetics (Llandro et al., 2010; Wang and Li, 2008), and electric field effects (Allen et al., 2007; Chen et al., 2011). A lot of these technologies are complicated to use at point-of-care: they require sophisticated laboratory equipment and laboratory technicians to operate. The biological samples measured by these platforms also often need extra processing, for example separating serums from whole blood samples. These requirements contribute to relatively expensive diagnostic cost and slow turnaround time, in addition to being bulky and immobile (Kricka, 1998; Tudos et al., 2001). These barriers limit the applications of emerging new platforms in resource-limited settings, such as in Africa and rural Asia, and also in non-clinical settings such as in homes, offices, or schools. On the other hand, commercially available strip tests, such as home pregnancy tests or Hepatitis tests, are simple to use and relatively inexpensive. However, the assay results are often only binary, or qualitative in nature, limiting its usefulness for in-depth disease analysis or disease monitoring. In addition, some researchers have raised concerns regarding the accuracy of these tests (Adeyemi et al., 2013; Cole et al., 2004; Doshi, 1986).

A diagnostic platform that combines the convenience of a strip test and the quantitative nature of clinical laboratory tests will be crucial in areas where access to healthcare is scarce. It can also reduce the burden of healthcare facilities where laypeople are able check their own health status, without having to visit hospitals or clinics. In this paper, we introduce Eigen Diagnosis Platform (EDP): a portable, quantitative immune diagnostic platform that employs Giant Magnetoresistance (GMR) biosensors. It has a smartphone interface that is simple to operate, and has a result turnaround

* Corresponding author.
E-mail address: sxwang@stanford.edu (S.X. Wang).
[1] These authors contributed equally to this work.

http://dx.doi.org/10.1016/j.bios.2016.04.046
0956-5663/

time of only less than 15 min. The simple operation of EDP makes it user-friendly, eliminating the need for a trained laboratory technician to operate the device. EDP employs one-step immunoassay; to operate the test, only one-time user involvement at the beginning of each test is necessary. The platform is also designed to be affordable; each test costs less than US$4 (Table S1). The use of a smartphone allows test results to be recorded, monitored, and transferred to the cloud seamlessly.

The GMR biosensors used in EDP can be customized to detect multiple biomarkers for a range of applications. In this paper, to demonstrate the performance of EDP we measured total human immunoglobulin G and M (IgG and IgM) concentrations simultaneously in one chip. IgG antibodies are found in all bodily fluids (Hoffbrand and Moss, 2015; Kindt et al., 2006). They are the most common antibodies (80% of all antibodies) in the body. IgG antibodies are essential in fighting bacterial and viral infections. IgM antibody is the first type of antibodies made in response to an infection (Hoffbrand and Moss, 2015; Kindt et al., 2006). They also cause other immune system cells to destroy foreign substances. IgM antibody makes up about (5–10%) of all the antibodies in the human body. Monitoring of IgG and IgM antibody levels in the body are important to help diagnose health conditions such as immunodeficiency, infection, autoimmunity, and hypergammaglobulinemia (Buckley, 1987; Dispenzieri et al., 2001; Driessen and van der Burg, 2011).

2. Method

2.1. GMR biosensor

GMR biosensor chips were fabricated as previously described (Gaster et al., 2009; Osterfeld et al., 2008). The chip has dimensions of 1.2 cm × 1 cm. It has an array of 64 (8 × 8) GMR spin valve sensors. Each sensor occupies an area of 100 μm × 100 μm. In-plane spin valve sensors were deposited on Si/SiO_2 substrate. The thickness of each layer from bottom to top is of the type (thickness in nm): Ta (3)/seed layer (4)/PtMn (15)/CoFe (2)/Ru (0.85)/CoFe (2)/Cu (2.3)/CoFe (2)/Cu (1)/Ta (4). The structure was passivated with SiO_2 (10)/Si_3N_4 (20)/SiO_2 (10) to protect the sensors from direct exposure to fluids. The mean resistances of GMR sensors used in the experiment were 1.86 K Ohms with the standard deviation of 73 Ω. The magnetoresistance ratio of the GMR sensors were 4%.

2.2. Sensor surface functionalization

Surface functionalization was done similarly as previously described (Kim et al., 2013). The GMR biosensor chips were triple washed with acetone, methanol, and isopropyl alcohol solution, then blow dried. The chips were exposed to oxygen plasma (PDC-32G Basic Plasma Cleaner, Harrick Plasma) for 1 min to remove remaining organic contaminants. A solution of 1% poly(allylamine hydrochloride) in deionized water was incubated on the chip for 5 min. The chips were then rinsed with deionized water, and heated up to 120 °C on a hotplate. After letting the chip to cool down to room temperature, a solution of 2% poly(ethylene-alt-maleic anhydride) was incubated on the chip for 5 min. The chip was then washed with deionized water, and a 1:1 mixture of 1-ethyl-3-(3-dimethylaminopropyl) carbodiimide hydrochloride (EDC) and N-hydroxysuccinimide (NHS) was incubated on the chip for one hour, then washed with deionized water.

2.3. Capture probe immobilization

The GMR biosensors were spotted with droplets of IgG or IgM capture antibodies. Bovine serum albumin (BSA) was spotted as a negative control. Biotinylated BSA (biotin-BSA) was spotted as a positive control and as a trigger to start data acquisition. Four groups of sensors in a same chip were spotted with 0.8 mg/ml of goat anti-human IgG Fc polyclonal antibody (RnD Systems, G-102-C), 0.8 mg/ml goat anti-human IgM Fc polyclonal antibody (RnD Systems, G-105-C), 1% bovine serum albumin (BSA) solution in phosphate buffered saline (PBS), and 0.1% biotin-BSA in PBS solution. Robotic nanopipetter machine (Scienion) was programmed to spot about 1.5 nL of solution per individual sensor in the GMR biosensor array. The prepared chip was incubated overnight at 4 °C in a humidity chamber. Subsequently, the sensor chip was washed and blocked with 2% BSA in PBS solution for one hour. After blocking, it was washed before use.

2.4. Detection of GMR biosensor signal

GMR biosensors have flicker noise (Hardner et al., 1993). If a readout signal is located at the low frequency, the signal is disturbed by the noise. To reduce the effect by the flicker noise from the GMR biosensor, the signal of interest is extracted by implementing the double modulation technique (de Boer et al., 2007; Han et al., 2007; T. Aytur, 2002). The double modulation is implemented by applying both sinusoidal electric voltage (fc) to the GMR biosensor and external sinusoidal magnetic field (ff). As the sinusoidal voltage (fc) and external magnetic field (ff) excite the GMR biosensors, the frequency spectrum of the output current contains primarily a carrier tone at fc and side tones at fc ± ff. The flicker noise of the sensor is modulated around fc, and the signal of interest is located at fc ± ff as shown in Fig. S2 (b).

2.5. Sensing scheme and signal acquisition

To detect an analyte of interest, EDP employs one-step magnetic sandwich immunoassay on the surface of the GMR biosensor (Fig. 2). A capture antibody that binds specifically to an analyte of interest is immobilized on the sensor surface. A sample mixture to be analyzed which has been mixed with analyte-specific biotinylated detection antibodies and streptavidin-coated MNPs (Miltenyi) is transferred into the reaction chamber on the sensor. An external magnetic field driven by one-inch Helmholtz coil generates magnetic fringing field from MNPs. When sandwiches of antibody-analyte-antibody-MNPs assemble on the sensor surface, the fringing magnetic field induces changes in the magnetoresistance of the GMR biosensor. GMR biosensor is a proximity-based sensor (Hall et al., 2010a); only the fringing field from MNPs that are immobilized on the sensor surface contributes to the change of resistance.

2.6. One-step wash-free immunoassay

To perform sample measurement, 25 μL of a mixture of diluted human IgG and IgM antibodies in 0.05% Tween 20 in PBS buffer (Sigma Aldrich) was mixed with 25 μL of streptavidin-coated superparamagnetic MNPs (Miltenyi, 130-048-101, 46 nm in diameter) and 5 μL mixture of 20 μg/ml of biotinylated anti-IgG Fc detection antibody (Jackson Immunoresearch) and 20 μg/ml of biotinylated anti-IgM Fc detection antibody (Jackson Immunoresearch). The mixture was mixed well, and then added into the reaction well on the chip. The sandwich between the capture probe, target analyte, detection antibody, and MNPs self-assembled on the sensor surface, giving rise to positive sensor signals (Fig. 1). With the one-step assay approach, no washing step is required, and assay runtime can be significantly reduced.

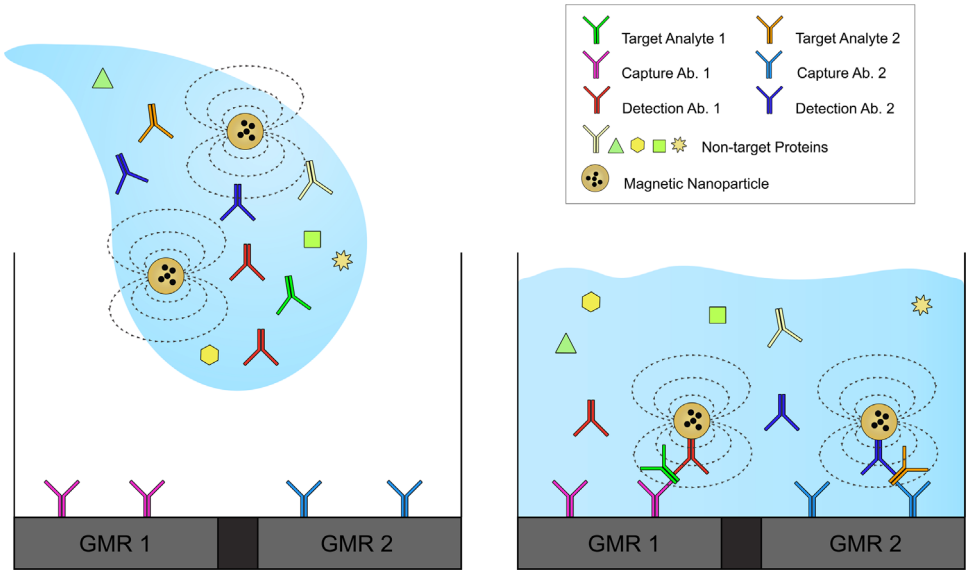

Fig. 1. The one-step wash-free assay. A mixture of sample to be analyzed (human IgG and IgM antibodies), detection antibodies, and MNPs are mixed well, and transferred into the reaction well on the GMR biosensor cartridge. The immobilized capture antibody, target analyte, detection antibody, and MNPs self-assemble on the sensor surface. Each individual sensor on the chip can be functionalized with a different capture probe, allowing measurement of multiple biomarkers in one test. An external magnetic field biases the MNPs, creating a directional magnetic fringing field. The fringing field changes the magnetoresistance of the GMR biosensor, resulting in a positive signal.

3. Results and discussions

3.1. Eigen Diagnosis Platform

EDP consists of three primary components: the reader station, disposable cartridge, and smartphone interfacing (Fig. 2). The cartridge houses the GMR biosensor chip which contains an array of 8×8 GMR magnetic sensors (Fig. S1). When the cartridge is inserted into the reader station, the reader station detects the magnetic sensors on the cartridge and records the electrical resistance in each sensor in real-time. The smartphone analyzes the data from the reader station, and displays it in a user-friendly format. The total cost per test including the GMR biosensor chip, bioreagents, and magnetic nanoparticles (MNPs) in high volume is less than US$4 (Table S1). The electronic parts composing the reader station cost less than US$120 in high volume (Table S2).

Fig. 2. The Eigen Diagnosis Platform (EDP). The EDP consists of three parts: a disposable cartridge, a reader station, and a smartphone running the Eigen Diagnosis App (shown on the smart phone screen). The reader acquires biological signals from the GMR biosensor in the cartridge, and transfers the data to the smartphone for signal processing.

3.2. Reader station

The Data Acquisition (DAQ) board in the reader station has two direct digital synthesis (DDS) chips (Analog Devices, AD9833). The two DDS chips provide sinusoidal excitations to an external one-inch Helmholtz coil and the GMR biosensor. Therefore, the electric current flowing through the GMR biosensor is double modulated: it is excited by both the coil and the voltage across GMR biosensors.

To get the signals from the GMR sensors, a carrier tone subtraction was performed at the hardware and software levels to amplify the subtracted signals (residual fc, fc $\pm$ ff). On the power amplifier board, an LC tank (Lee, 1988) is used to reduce the power consumption when driving the one-inch Helmholtz coil.

3.2.1. Carrier tone suppression

To detect the change of the modulated signal caused by biological reactions, the sensor output signal should be amplified with a large factor to be recognized by the analog-to-digital converter (ADC) on the board. However, the output signal from the sensor often cannot be directly amplified with a large factor because of the voltage headroom of the system and the reference voltage of the ADC. So the carrier tone suppression circuit (Hall et al., 2010b) and algorithm were implemented. The suppression circuit has an array of 16 resistors ranging from 1.65 K Ohms to 1.96 K Ohms on the reader board. The algorithm finds one matching resistor per individual biosensor in the chip that has the most similar resistance value compared to the resistance of the biosensor. The carrier tone suppression circuit shown in Fig. 3

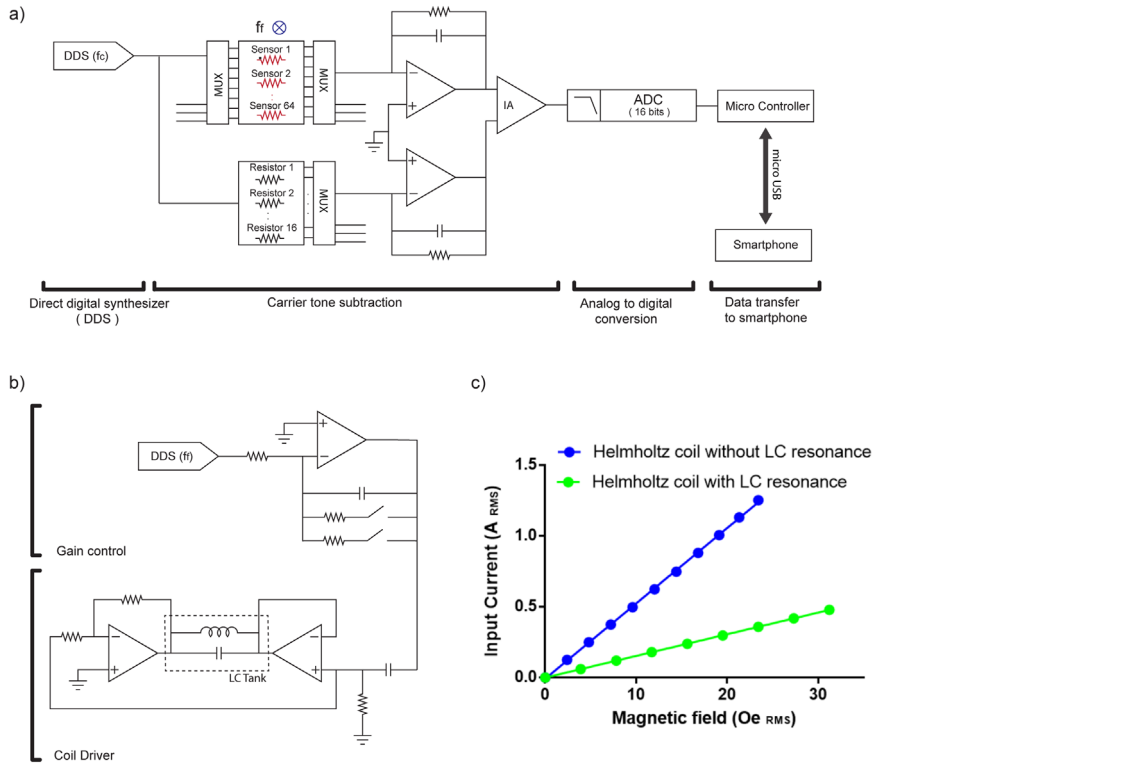

Fig. 3. (a) Readout circuit schematic of EDP. The mainboard is composed of four parts: Direct digital synthesizer (DDS) chips generate a carrier tone (fc) and a magnetic field tone (ff). A carrier tone subtraction circuit subtracts the majority of the carrier tone and magnifies the rest of the signal. Analog to digital conversion circuit has an anti-aliasing filter in the front and converts analog signals into 16-bit digital signal. A data transfer circuit transfers the raw data to a smartphone via micro USB. (b) Coil driver schematic of EDP Diagram. Coil driver can generate two different magnitudes of magnetic fields for MR calibration of each GMR biosensor. Power amplifiers of the coil driver circuit drive an LC tank. The LC tank is composed of a coil (to generate magnetic field) and ceramic capacitors. (c) Measured magnetic field versus input current of the LC tank and one-inch Helmholtz coil.

(a) subtracts the carrier tone signal with the selected resistors and suppresses the carrier tone at least by −31.21 dB when the resistances are in the range of the known fabrication variation.

The carrier tones at the outputs of the two preamplifiers (Texas Instruments, OPA209) in the carrier tone suppression circuit have similar magnitudes because a proper resistor selected by the system for the carrier tone subtraction. So, the instrumentation amplifier (Analog Devices, AD8221) can amplify the differential signals with the amplification factor of 17.83. The anti-aliasing filter stage with an amplification factor of 4.65 were implemented prior to the analog-to-digital conversion stage to prevent possible aliasing effect caused by intermodulation and harmonics. The 16-bit analog-to-digital conversion chip (Analog Devices, ADS8330) samples the output signal at 44.4 KHz rate and transfers the digitized data points to a microcontroller (Microchip, PIC24EP512GU810). The microcontroller transfers the raw data to a smartphone (Samsung Galaxy S3 Mini GT-I8200) through the micro-USB for signal processing.

3.2.2. *Magnetic field generation: LC tank*

To generate the external magnetic field, alternating current is supplied to the one-inch Helmholtz coil. However, the majority of the power was consumed to supply the current. To reduce the power consumption, the coil which has an inductance of 420 μH is connected in parallel to a 300 μF ceramic capacitor to form an LC tank (Fig. 3(b)). With the LC tank, the alternating current at the resonant frequency of the LC tank circulates between the coil and the capacitor. Without the LC tank, all of the electric current flowing through the coil sinks to the ground. Fig. 3(c) shows the comparison between the steady state alternating input current and the generated magnetic field density on the Helmholtz coil with and without the LC tank. Using the LC tank, the power consumption of the external coil when generating the same magnitude of magnetic flux density is reduced by 71%.

For implementing the LC tank, the sinusoidal signal for the resonant frequency of the LC tank was generated by a DDS chip (Texas instruments, AD9833) in the board. As shown in Fig. 3(b), the sinusoidal signal was fed through a negative feedback circuit where single pole double throw (SPDT) switch (Vishay Siliconix, DG4157) is used to control the magnitude of the magnetic field. To maximize the voltage swing across the LC tank, two power amplifiers (Texas instruments, OPA569) were used for bridge tied load configuration.

3.3. *The smartphone app*

Eigen Diagnosis App for android smartphones was designed to analyze the biological data and to guide users. When the reader station is connected to the android smartphone loaded with the Eigen Diagnosis App via a micro-USB, the app requests users to insert a cartridge into the station by displaying the message on the screen as shown in Fig. 4. The station checks if the cartridge has been inserted by attempting to measure the resistance of the sensors. Then, the app displays a message asking users to prepare a sample mixture. At the same time, the platform measures magnetoresistances (MRs) at two different magnetic fields for calibration of the sensors. After the calibration, the app displays “Add Sample” message until users add the sample. When the sample is added through the opening at the top of the EDP station, the platform monitors positive signals from the biotin-BSA coated sensors to trigger the acquisition of signals from other sensors for 10 min. During the 10 min, the station acquires the raw data from the sensors and sends them to the app via the micro USB. Then the app processes the raw data to extracts MR changes caused by the

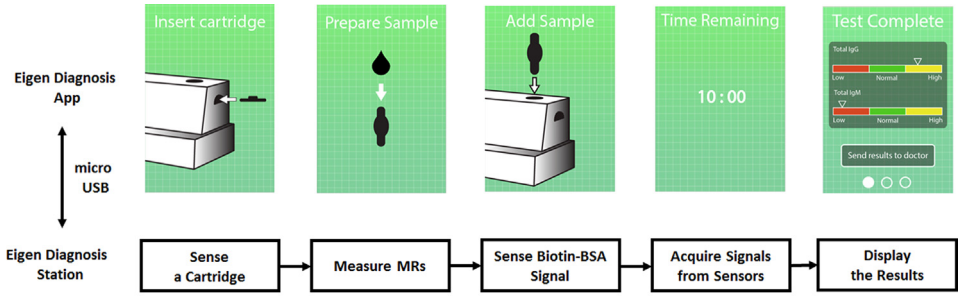

Fig. 4. Block diagram of the test process of the Eigen Diagnosis app that leads users through the tests. When a smartphone loaded with the Eigen Diagnosis app is connected with micro USB, the app displays "Insert Cartridge" and the station checks continuously if a cartridge is inserted. Once a cartridge is sensed, the app displays "Prepare Sample" on the screen and the station calibrates MR characteristics of each GMR biosensor. After the calibration is completed, the app shows "Add Sample" on the screen. When a user adds the prepared sample and the rise of biotin-BSA is sensed, the app counts 10 min. After the 10 min, the result is displayed on the app screen with the bar graphs.

antibody-analyte-antibody-MNPs sandwiches on the sensors.

To suppress the spectral leakage due to the discontinuity between the beginning of the signal and the end of the signal for FFT, the app multiplies the signal with Hanning window (Harris, 1978) (8192 points) before performing Fast Fourier Transform (Cooley et al., 1969) (FFT). The smartphone performs FFT on the raw data, and acquires the magnitude of the carrier tone (fc) and the side tones (fc $\pm$ ff) of each sensor. Since the carrier tone has the subtracted magnitude from the original signal due to the carrier subtraction circuit shown in Fig. 3(a), the real magnitude of carrier tone can be recovered based on the resistor value used for the carrier subtraction.

To compensate for the temperature change during the test, the app extracts the temperature correction factors from carrier tone during the measurement, and the app adjusts the corresponding side tone with the correction factors (Hall et al., 2010b). The MR characteristic of each sensor is calibrated in the beginning of the test as shown in Fig. S3(a) and the ΔMRs at each time point are corrected with the MR correction factors (Hall et al., 2010b).

EDP measures the rates of biological bindings instead of the steady-state signals because one-step wash-free immunoassay is employed and the signals have not reached steady states within 10 min. Since the slopes of the acquired signals from the one-step wash-free immunoassay are approximately linear for the first 10 min as shown in Fig. S3 (b), the initial slopes can be measured to distinguish the concentrations of the analytes. The app decides when slopes are measured by sensing the rise of biotin-BSA (positive control) signal. When the biotin-BSA signals reach 75 ppm, the app starts to acquire the signal from all of the GMR biosensors for 10 min. Then the app applies a linear regression algorithm to the signal from each spotted sensor as shown in Fig. S3 (c), and a representing slope of each target of interest is calculated by Huber penalty function (Lambert-Lacroix and Zwald, 2011; Vandenberghe, 2002) as shown in Fig. S3 (d) to minimize the effect caused by binding variations or possibly faulty sensors.

3.4. Multiplexed detection of target analytes and assay results

Each sensor in the cartridge is capable of detecting one target analyte of interest (antibody or antigen). To detect an analyte, the EDP uses a magnetic sandwich assay mechanism directly on top of the GMR biosensor. To demonstrate the multiplexing capability, we measured human IgG and IgM antibody concentrations simultaneously in one chip. Capture antibodies that are specific to human IgG or IgM antibodies are immobilized on the surface of each sensor. The capture antibodies act as "traps" that immobilize free-floating human IgG or IgM antibodies in the sample. To complete the sandwich structure, detection antibodies specific to human IgG or IgM antibodies attach to the immobilized target analytes. The detection antibodies have been labeled with biotin, so streptavidin-coated MNPs will bind to them, completing the antibody-analyte-antibody-MNPs sandwiches. The MNPs, biased by the external magnetic coil, create magnetic fringing fields that are detected by the GMR biosensors underneath the sandwich structure. The higher the concentration of the target analytes of interest, the more the target analytes are captured onto the sensor surface, and the more MNPs attach to the captured analytes. This chain of binding events leads to a positive signal reading from the sensor. Because the sensor is only affected by MNPs that are in proximity to the sensor surface, MNPs that are not captured to the surface (i.e., are free-floating) do not contribute to the positive sensor signal (Hall et al., 2010a). To eliminate the effect of non-specific binding, the signals from IgG and IgM sensors are subtracted by BSA-coated negative control (background) signals.

The multiplexed measurements of human IgG and IgM antibodies are shown in Fig. 5(a, b). After the mixtures are inserted, the sandwich structures start to self-assemble. In the 10-minute time window of measurement, readout GMR biosensor signals increase approximately linearly. Linear regression is used to obtain the rate of signal growth. When analyte concentrations are higher, more antibody-analyte-antibody-MNPs sandwich bindings occur on the surface of the GMR biosensors at a given time, resulting in faster growth of signals.

are obtained by calculating the standard deviations of the signals from duplicate sensors at the particular time points.

The averages of the linearly-regressed slopes from IgG or IgM sensors at various concentrations are plotted to obtain the standard curves of the multiplexed assays (Fig. 5(c)). The standard deviations indicate the slope variations. The multiplexed IgG and IgM antibodies detection has sensitivities of 10 ng/ml (0.07 nanomolar) and 50 ng/ml (0.33 nanomolar), respectively, with two orders of magnitude of dynamic range. The assay sensitivities are limited by the background signal levels (the dashed lines), which are defined as the mean of the zero-analyte signals plus two standard deviations. To show the capability of the platform in measuring real biological samples, we measured unprocessed whole blood samples from a healthy volunteer at three different serial dilutions (Fig. S5). EDP can successfully distinguish between different blood dilutions–a sample with a lower dilution is shown to have a higher signal than a sample with a higher dilution, as expected.

4. Conclusions

Compared to the standard clinical laboratory, EDP is portable, allowing diagnostics at point-of-care. In contrast to a clinical laboratory assay which is labor intensive and takes hours to complete, EDP can obtain results in less than 15 min with one-time user involvement. In addition, EDP can detect various target

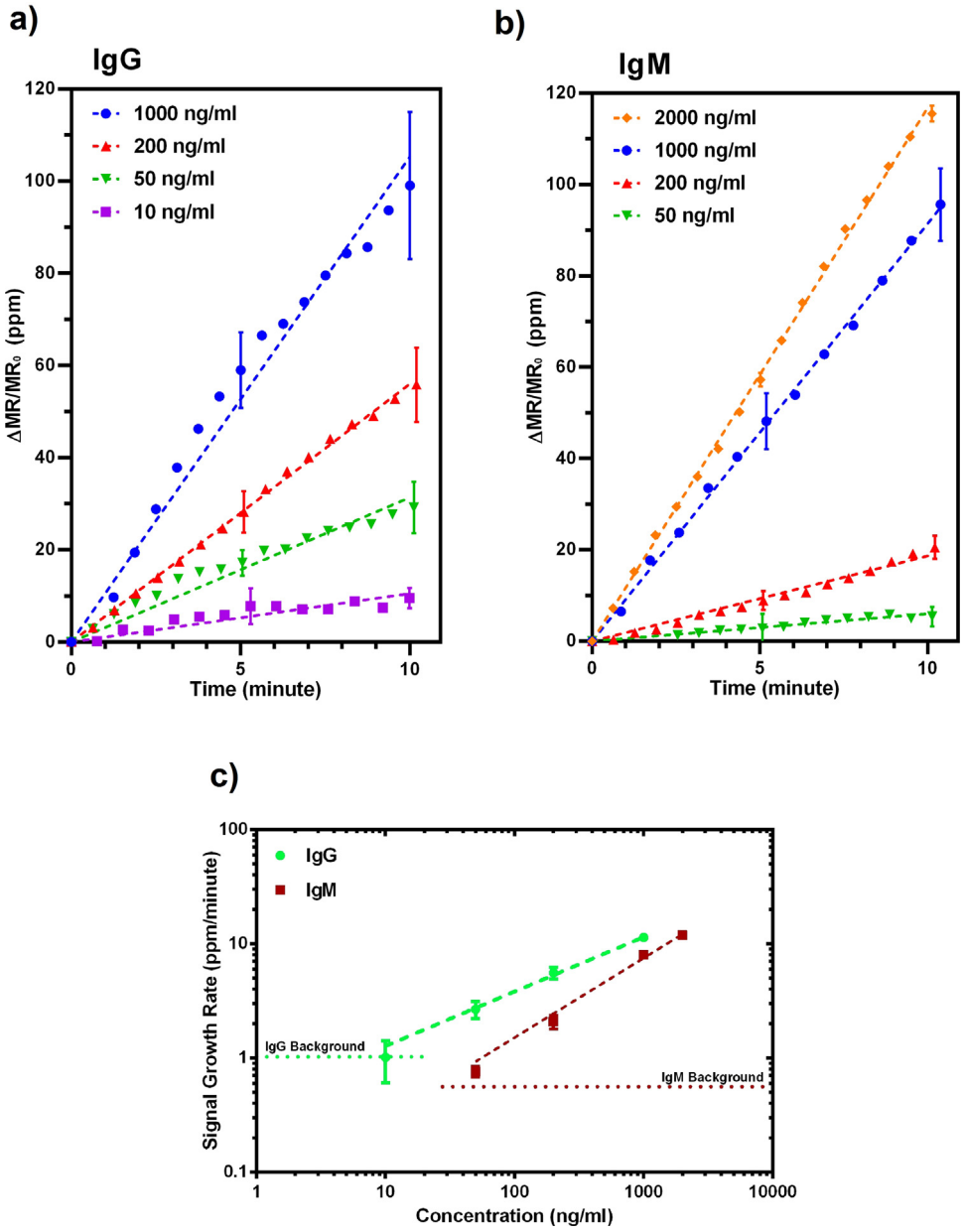

Fig. 5. The average signal increase over time as measured using the EDP from (a) IgG and (b) IgM sensors at various concentrations over the ten-minute measurement period. As can be observed, signal increases approximately linearly. Signal slopes are obtained by linear regression, and are used to quantify the concentrations of target analytes in the sample. (c) Calibration curves of multiplexed IgG and IgM assays. The background signal levels are plotted as dashed lines. The error bars in (a) and (b) indicate standard deviations of the signals from duplicate sensors at the particular time points. The error bars in (c) indicate standard deviations of the signal growth rates (slopes) of duplicate sensors from t=0 to t=10 min.

analytes by immobilizing different capture probes on different sets of GMR biosensors as we demonstrated in the simultaneous detection of total human IgG and IgM antibodies. With the multiplexing capability of the GMR biosensors, a wealth of health information can be extracted just from a drop of whole blood.

We have demonstrated a portable GMR biosensor platform with smartphone integration that can open up many use cases where individuals have the means to check important health markers without the need to visit hospitals or clinical laboratories that may be far away or even unavailable. By only forwarding the results to doctors when the attention is required while the normal results are directly integrated into the users' medical records, we can reduce doctors' workload, and streamline the medical workflow. This will enable a new healthcare paradigm whereby individuals can save time by performing medical tests at home, and adjust their own lifestyles by monitoring their health conditions on demand, while doctors can spend their time more efficiently. The use of EDP is not limited to only personal diagnostics. Looking forward, Eigen Diagnosis App can be used to accumulate the levels of biomarkers of interest for many individuals recorded over weeks, months, or even years in a database and new insights into human health and the immune system can be gleaned with "big data" approaches (Kayyali et al., 2013).

In a future development, the idea of detecting different types of antibodies can be expanded to measure the isotypes of specific antibodies to certain diseases. The human immune system generates different amounts of specific IgG and IgM antibodies depending on the status of diseases. For example, the existence of IgG and IgM antibodies to specific Hepatitis virus antigens can indicate an infection status (acute or chronic) (Centers for Disease

Control and Prevention, 2006; World Health Organization Department of Epidemic and Pandemic Alert and Response, 2002). More detailed information of antibody composition in a drop of blood can help understand the immune status more in-depth, leading to a more personalized treatment.

Conflict of interest

SXW has related patents or patent applications assigned to Stanford University and out-licensed for potential commercialization. SXW has stock shares in MagArray, Inc., which has licensed relevant patents from Stanford University for commercialization of GMR biosensor chips.

Acknowledgement

This work was supported by Stanford Center for Magnetic Nanotechnology and Skippy Frank Translational Fund. We acknowledge XPRIZE Foundation and Nokia Sensing XCHALLENGE competition for motivating the design of the Eigen Diagnosis Platform which won Distinguished Prize Award. JC acknowledges the STX Foundation fellowship, and DJBB acknowledges Stanford Bio-X Graduate Fellowship. The authors would like to thank Professor Samuel So at Stanford University Asian Liver Center for fruitful discussion and Jon Derman Harris for designing the artwork of the Eigen Diagnosis App.

Appendix A. Supporting information

Supplementary data associated with this article can be found in the online version at http://dx.doi.org/10.1016/j.bios.2016.04.046.

References

Adeyemi, A., Omolade, O., Raheem-Ademola, R., 2013. Immunochromatographic testing method for Hepatitis B, C in blood donors. J. Antivir. Antiretrovir. S3, 2.
Allen, B.L., Kichambare, P.D., Star, A., 2007. Carbon nanotube field-effect-transistor-based biosensors. Adv. Mater. 19 (11), 1439–1451.
Kayyali, B., Knott, D., Kuiken, S.V., 2013. The big-data revolution in US health care: Accelerating value and innovation.
Buckley, R., 1987. Immunodeficiency diseases. J. Am Med. Assoc. 258 (20), 2841–2850.
Centers for Disease Control and Prevention, 2006. Prevention of Hepatitis A through active or passive immunization: recommendations of the Advisory Committee on Immunization Practices (ACIP). MMWR.
Chen, K.-I., Li, B.-R., Chen, Y.-T., 2011. Silicon nanowire field-effect transistor-based biosensors for biomedical diagnosis and cellular recording investigation. Nano Today 6 (2), 131–154.
Cole, L.A., Khanlian, S.A., Sutton, J.M., Davies, S., Rayburn, W.F., 2004. Accuracy of home pregnancy tests at the time of missed menses. Am. J. Obstet. Gynecol. 190 (1), 100–105.
Cooley, J.W., Lewis, P.A.W., Welch, P.D., 1969. The fast fourier transform and its applications. Educ. IEEE Trans. 12 (1), 27–34.
de Boer, B.M., Kahlman, J.A.H.M., Jansen, T.P.G.H., Duric, H., Veen, J., 2007. An integrated and sensitive detection platform for magneto-resistive biosensors. Biosens. Bioelectron. 22 (9–10), 2366–2370.
Dispenzieri, A., Gertz, M.A., Therneau, T.M., Kyle, R.A., 2001. Retrospective cohort study of 148 patients with polyclonal gammopathy. Mayo Clin. Proc. 76 (5), 476–487.
Doshi, M.L., 1986. Accuracy of consumer performed in-home tests for early pregnancy detection. Am. J. Public Health 76 (5), 512–514.
Driessen, G., van der Burg, M., 2011. Educational paper. Eur. J. Pediatr. 170 (6), 693–702.
Fan, X., White, I.M., Shopova, S.I., Zhu, H., Suter, J.D., Sun, Y., 2008. Sensitive optical biosensors for unlabeled targets: A review. Anal. Chim. Acta 620 (1–2), 8–26.
Gaster, R.S., Hall, D.A., Nielsen, C.H., Osterfeld, S.J., Yu, H., Mach, K.E., Wilson, R.J., Murmann, B., Liao, J.C., Gambhir, S.S., Wang, S.X., 2009. Matrix-insensitive protein assays push the limits of biosensors in medicine. Nat. Med. 15 (11), 1327–1332.
Haes, A.J., Van Duyne, R.P., 2002. A nanoscale optical biosensor: sensitivity and selectivity of an approach based on the localized surface plasmon resonance spectroscopy of triangular silver nanoparticles. J. Am. Chem. Soc. 124 (35), 10596–10604.
Hall, D.A., Gaster, R.S., Lin, T., Osterfeld, S.J., Han, S., Murmann, B., Wang, S.X., 2010a. GMR biosensor arrays: A system perspective. Biosens. Bioelectron. 25 (9), 2051–2057.
Hall, D.A., Gaster, R.S., Lin, T., Osterfeld, S.J., Han, S., Murmann, B., Wang, S.X., 2010b. GMR biosensor arrays: A system perspective. Biosens. Bioelectron. 25 (9), 2051–2057.
Han, S.-J., Yu, H., Murmann, B., Pourmand, N., Wang, S.X., 2007. A High-Density Magnetoresistive Biosensor Array with Drift-Compensation Mechanism. Solid-State Circuits Conference, 2007. ISSCC 2007. Digest of Technical Papers. IEEE International, pp. 168–594.
Hardner, H.T., Weissman, M.B., Salamon, M.B., Parkin, S.S.P., 1993. Fluctuation-dissipation relation for giant magnetoresistive 1//textit{f} noise. Phys. Rev. B 48 (21), 16156–16159.
Harris, F.J., 1978. On the use of windows for harmonic analysis with the discrete Fourier transform. Proc. IEEE 66 (1), 51–83.
Hoffbrand, V., Moss, P.A.H., 2015. Hoffbrand's Essential Haematology, 7 ed. Wiley-Blackwell,.
Kim, D., Marchetti, F., Chen, Z., Zaric, S., Wilson, R.J., Hall, D.A., Gaster, R.S., Lee, J.-R., Wang, J., Osterfeld, S.J., Yu, H., White, R.M., Blakely, W.F., Peterson, L.E., Bhatnagar, S., Mannion, B., Tseng, S., Roth, K., Coleman, M., Snijders, A.M., Wyrobek, A.J., Wang, S.X., 2013. Nanosensor dosimetry of mouse blood proteins after exposure to ionizing radiation. Sci. Rep. 3, 2234.
Kindt, T.J., Osborne, B.A., Goldsby, R.A., 2006. Kuby Immunology, 6 ed. W. H. Freeman & Company,.
Kneipp, J., Kneipp, H., Wittig, B., Kneipp, K., 2010. Novel optical nanosensors for probing and imaging live cells. Nanomed.: Nanotechnol., Biol. Med. 6 (2), 214–226.
Kricka, L.J., 1998. Miniaturization of analytical systems. Clin. Chem. 44 (9), 2008–2014.
Lambert-Lacroix, S., Zwald, L., 2011. Robust. Regres. Huber's criterion Adapt. lasso Penal., 1015–1053.
T.H., Lee, 1988. The Design of CMOS Radio-Frequency Integrated Circuits.
Llandro, J., Palfreyman, J.J., Ionescu, A., Barnes, C.H.W., 2010. Magnetic biosensor technologies for medical applications: a review. Med Biol. Eng. Comput. 48 (10), 977–998.
Osterfeld, S.J., Yu, H., Gaster, R.S., Caramuta, S., Xu, L., Han, S.-J., Hall, D.A., Wilson, R. J., Sun, S., White, R.L., Davis, R.W., Pourmand, N., Wang, S.X., 2008. Multiplex protein assays based on real-time magnetic nanotag sensing. Proc. Natl. Acad. Sci. 105 (52), 20637–20640.
T. Aytur, P.R.B.a.B.B., 2002. An Immunoassay Platform Based on CMOS Hall Sensors. Solid-State Sensor, Actuator and Microsystems Wokshop, pp. 126–129, Hilton Head Island, SC.
Tudos, A.J., Besselink, G.A.J., Schasfoort, R.B.M., 2001. Trends in miniaturized total analysis systems for point-of-care testing in clinical chemistry. Lab Chip 1 (2), 83–95.
S.B.a, Vandenberghe. L., 2002. Convex Optimization.
Wang, S.X., Li, G., 2008. Advances in giant magnetoresistance biosensors with magnetic nanoparticle tags: review and outlook. Magn. IEEE Trans. 44 (7), 1687–1702.
World Health Organization Department of Epidemic and Pandemic Alert and Response, 2002. Hepatitis B. World Health Organization,, Geneva, Switzerland.